



THE UNIVERSITY *of* EDINBURGH

## Edinburgh Research Explorer

### **Sonochemical oxidation of piroxicam drug: Effect of key operating parameters and degradation pathways**

**Citation for published version:**

Lianou, A, Frontistis, Z, Chatzisyseon, E, Antonopoulou, M, Konstantinou, I & Mantzavinos, D 2017, 'Sonochemical oxidation of piroxicam drug: Effect of key operating parameters and degradation pathways', *Journal of chemical technology and biotechnology*, vol. 93, no. 1, pp. 28-34.  
<https://doi.org/10.1002/jctb.5346>

**Digital Object Identifier (DOI):**

[10.1002/jctb.5346](https://doi.org/10.1002/jctb.5346)

**Link:**

[Link to publication record in Edinburgh Research Explorer](#)

**Document Version:**

Peer reviewed version

**Published In:**

Journal of chemical technology and biotechnology

**General rights**

Copyright for the publications made accessible via the Edinburgh Research Explorer is retained by the author(s) and / or other copyright owners and it is a condition of accessing these publications that users recognise and abide by the legal requirements associated with these rights.

**Take down policy**

The University of Edinburgh has made every reasonable effort to ensure that Edinburgh Research Explorer content complies with UK legislation. If you believe that the public display of this file breaches copyright please contact [openaccess@ed.ac.uk](mailto:openaccess@ed.ac.uk) providing details, and we will remove access to the work immediately and investigate your claim.



**Sonochemical oxidation of piroxicam drug: Effect of key operating parameters and degradation pathways**

Athina Lianou,<sup>a</sup> Zacharias Frontistis,<sup>a\*</sup> Efthalia Chatzisyneon,<sup>b</sup> Maria Antonopoulou,<sup>c</sup> Ioannis Konstantinou,<sup>d</sup> and Dionissios Mantzavinos<sup>a</sup>

(a) Department of Chemical Engineering, University of Patras, Caratheodory 1, University Campus, GR-26504 Patras, Greece

(b) Institute for Infrastructure and Environment, School of Engineering, The University of Edinburgh, Edinburgh EH9 3JL, United Kingdom

(c) Department of Environmental & Natural Resources Management, University of Patras, 2 Seferi St., GR-30100 Agrinio, Greece

(d) Department of Chemistry, University of Ioannina, GR-45110 Ioannina, Greece

\* Corresponding author:

Email: zfrontistis@chemeng.upatras.gr; Tel.: +302610996137; Fax: +302610969532

## Abstract

**BACKGROUND:** Piroxicam (PRX) is a non-steroidal anti-inflammatory drug (NSAID) commonly used to relieve pain and swelling of conditions like arthritis. PRX has been extensively detected in seawater, surface, and sewage waters worldwide and therefore its efficient treatment is an issue of emerging concern. In this work, the sonochemical degradation of PRX was investigated.

**RESULTS:** All experiments were conducted at constant ultrasound frequency of 20 kHz while the following range of experimental conditions was investigated: initial PRX concentration 320–960 µg/L, ultrasound power density 20–60 W/L, temperature 20–60 °C, reaction time up to 60 min. The effect of different water matrices, namely surface water (SW), bottled water (BW), ultrapure water (UPW) and humic acid (HA) aqueous solution on process efficiency was also explored. It was found that PRX degradation reached 96% after only 10 min of treatment at the best conditions (i.e.  $[PRX]_0 = 320$  mg/L, 20°C, 36 W/L) assayed. Power density could positively affect PRX degradation. Nevertheless, PRX degradation decreased when its initial concentration and the temperature of the bulk liquid was increased. PRX degradation was found to decrease, in different water matrices, in the order: UPW > 5 mg/L HA > BW > 10 mg/L HA > SW. High resolution mass spectrometry analysis revealed that fourteen transformation by-products (TBPs) were formed and subsequently degraded during treatment while the PRX degradation pathways were also elucidated.

**CONCLUSION:** At the optimal operating conditions assayed, PRX was efficiently degraded after about 10 min of sonochemical oxidation, thus rendering it a promising technology for the treatment of xenobiotics

39

40   **Keywords:** NSAIDs; wastewater treatment; ultrasound; pharmaceuticals; intermediate products

## 1. Introduction

Piroxicam (PRX) is a non-steroidal anti-inflammatory drug (NSAID) commonly used to relieve pain and swelling of conditions like arthritis. NSAIDs, including PRX, have been extensively detected in seawater, surface, and sewage waters worldwide,<sup>1-3</sup> since these are among the most frequently used drugs (painkillers, antipyretics, treatment of inflammations and prevention of myocardial infarction). The presence of such drugs, even at low concentrations (from ng/L to mg/L), can have a significant impact on the aquatic and terrestrial systems, and therefore this is an issue of emerging concern.<sup>4</sup>

Excretion (from human and animal medical care) is the major source of water and soil pollution by drugs. These are excreted as unchanged or metabolites, which after disposal to municipal sewage systems find their way to the environment.<sup>3</sup> Wastewater treatment plants (WWTPs) have been mainly designed to remove suspended solids and organic content while their effect on the removal of micropollutants may be, in most cases, negligible.<sup>1</sup> Therefore, when drugs enter conventional biological WWTPs, only a small fraction is removed and residual amounts are released into the terrestrial and aquatic environment, causing major environmental and health concerns. Due to inadequacy of current WWTPs to completely remove such contaminants, additional or alternative processes should be applied to support existing treatment facilities and increase their efficiency.

Sonochemical oxidation is an advanced oxidation process (AOP), which has gained considerable attention over the past decades for the treatment of several trace pollutants, including pharmaceutical substances.<sup>5-7</sup> Sonochemical oxidation is based on the in situ generation of powerful oxidizing agents, such as the hydroxyl radical. These are formed through the cyclic formation, growth and implosive collapse of bubbles that behave as hot-spot, micro-reactors.<sup>8,9</sup> At

sufficient contact time and proper operating conditions, sonochemical oxidation may mineralize all organic carbon to CO<sub>2</sub>, which is the most stable end product of chemical oxidation. The sonochemical degradation of various NSAIDs, such as ibuprofen,<sup>10,11</sup> naproxen,<sup>12</sup> and diclofenac<sup>13-16</sup> has been investigated. Nevertheless, to the best of our knowledge, there is no study on the sonochemical degradation of PRX, a commonly used NSAID. In addition, unlike other drugs, the advanced oxidation of PRX has been merely explored. Specifically, there is only one study by Feng et al.,<sup>17</sup> who investigated the degradation of three NSAIDs, including PRX by means of ozone or H<sub>2</sub>O<sub>2</sub>/O<sub>3</sub> treatment. That study focused on determining the bio-availability of chemical intermediates formed in ozonated water onto a biofilm-supporting granular activated carbon.

The purpose of this work is to investigate the sonochemical oxidation of PRX, evaluate the effect of key operating parameters that can determine degradation rates and propose degradation pathways. Therefore, the following parameters, namely initial PRX concentration, power density, reaction time, water matrix, and temperature are studied. Transformation by-products are identified and a potential degradation pathway is proposed.

## **2. Materials and methods**

### **2.1 Materials**

Piroxicam (PRX) (C<sub>15</sub>H<sub>13</sub>N<sub>3</sub>O<sub>4</sub>S, CAS no: 36322-90-4) was supplied by Sigma–Aldrich and used as received. All experiments, unless otherwise stated, were performed in ultrapure water (UPW) with pH = 6.5 taken from a water purification system (EASYpureRF-Barnstead/Thermolyne, USA). Two more water matrices were employed for this study. One was a commercially available bottled water (BW) (pH = 7.5, 0.4 mS/cm conductivity containing 211 mg/L bicarbonate, 10 mg/L

chloride, 15 mg/L sulfate, 5 mg/L nitrate and 78 mg/L of various metal ions), and the other was surface water (SW) collected from a stream near the city of Athens, Greece (pH=7.8, 166 mg/L bicarbonate, 11 mg/ chloride, and 51 mg/L sulfate). Humic acid (HA, CAS number 1415-93-6) was purchased from Sigma–Aldrich. Sodium chloride (NaCl, CAS no: 7647-14-5) and sodium bicarbonate (NaHCO<sub>3</sub>, CAS no: 144-55-8), used as free radical scavengers, were purchased from Sigma-Aldrich.

## **2.2 Ultrasound irradiation**

A Branson 450 horn-type digital sonifier operating at a fixed frequency of 20 kHz and a variable power output up to 450W (nominal) was employed. Sonochemical oxidation took place in a cylindrical, double-walled, Pyrex vessel, which was open to the atmosphere. Ultrasound irradiation was emitted through a 1 cm in diameter titanium tip which was positioned in the middle of the vessel at a distance of 3 cm from the bottom. The working volume was 0.12 L and the actual power density emitted to the bulk solution was determined calorimetrically and it was found to be between 20 and 60 W/L. Temperature was kept at 20 °C, unless otherwise stated, by a temperature control unit. Most experiments were performed in duplicate and mean values, whose standard deviation never exceeded 5%. Samples of 1.2 mL were periodically taken from the reactor and analyzed as follows.

## **2.3 Chromatographic techniques**

High performance liquid chromatography (HPLC: Alliance 2695, Waters) was employed to monitor the concentration of PRX. Separation was achieved on a Kinetex XB-C18 100A column

(2.6  $\mu\text{m}$ , 2.1 mm  $\times$  150 mm) and a 0.5  $\mu\text{m}$  inline filter (KrudKatcher Ultra) both purchased from Phenomenex. The mobile phase consisting of 68:32 water:acetonitrile eluted isocratically at 0.35 mL/min and 45 °C, while the injection volume was 100  $\mu\text{L}$ . Detection was achieved through a photodiode array detector (Waters 2996 PDA detector, detection  $\lambda$  = 350 nm). The limit of detection was 3.52  $\mu\text{g/L}$ , and the limit of quantitation was 11.75  $\mu\text{g/L}$

LC-MS/TOF analysis was carried out on a system, consisted of a Dionex UHPLC Ultimate 3000 connected to a BRUKER micrOTOF Focus II mass spectrometer. Gradient methods were developed on a Thermo Scientific Acclaim<sup>TM</sup> RSLC 120 C18 column (protected by a guard from Waters) thermostated at 30° C, using a mixture of water/1mM ammonium formate and methanol as mobile phase at a flow rate of 0.3 mL/min. The elution starts with 1% methanol and progressively increases to 99% (methanol) at 10 min. At 12 min the initial conditions are reached and retained for 3 min (15 min). The micrOTOF Focus II was operated in both ionization modes (positive and negative) as follows: dry gas at 8 L/min, nebulizer press at 2.4 bar, dry heater at 200° C, hexapole RF at 100 Vpp and capillary voltage at 4500 V. Accurate mass measurements provided by micrOTOF Focus II mass spectrometer and the interpretation of fragments derived from in source Collision-induced Dissociation (isCID) was used for the structural assignment of transformation by-products (TBPs).

### **3. Results and discussion**

#### **3.1 Effect of initial PRX concentration**

The effect of initial PRX concentration, ranging from 320  $\mu\text{g/L}$  to 960  $\mu\text{g/L}$ , on its degradation rate was studied. Figure 1 shows PRX degradation as a function of treatment time at 36 W/L power



density, and constant temperature of 20 °C. Complete removal is achieved after 25 min of treatment for 640–960 µg/L PRX and this decreases to almost 10 min when initial PRX concentration is 320 µg/L. Data of Figure 1 are found to fit well a pseudo first-order reaction, which is in agreement with previous studies on sonochemical degradation of other NSAIDs, such as ibuprofen<sup>18</sup> and diclofenac<sup>14,15,19</sup>. In the inset graph of Figure 1 it is observed that the kinetic rate coefficients,  $k$ , decrease when the initial substrate concentration is increased. For example, rate coefficients are 0.1459 min<sup>-1</sup>, 0.1695 min<sup>-1</sup> and 0.2098 min<sup>-1</sup> when the initial PRX concentration is 960 µg/L, 640 µg/L and 320 µg/L, respectively. The fact that rate coefficient changes with varying PRX concentration implies that the reaction is not true first order although data fitting to first-order kinetics equation (i.e.  $\ln [PRX]_0/[PRX]=kt$ ) is good.

Figure 1.

### 3.2 Effect of power density

Ultrasound power is a key operating parameter that can substantially affect efficiency of sonochemical oxidation. Therefore, different power densities, ranging from 20 to 60 W/L, were applied for the degradation of 640 µg/L PRX and the results are shown in Figure 2. As seen conversion increases with increasing applied power. Not only this but, as shown in the inset graph of Figure 2, a nearly linear increase of PRX degradation with power density is observed. Specifically, reaction rate coefficients are 0.1157 min<sup>-1</sup> ( $r^2=0.9688$ ), 0.1695 min<sup>-1</sup> ( $r^2=0.9868$ ) and 0.1967 min<sup>-1</sup> ( $r^2=0.9921$ ) when power density is 20, 36 and 60 W/L, respectively. This increase of PRX degradation can be attributed to the fact that, at higher power levels, the transmittance of

ultrasonic energy into the reactor increases. As a result, a larger number of cavitation bubbles are formed and the pulsation and collapse of bubbles occur at a faster rate, thus increasing significantly the concentration of hydroxyl radicals generated, and the subsequent H<sub>2</sub>O<sub>2</sub> production in the liquid mixture, leading to enhanced organics degradation rates.<sup>20-22</sup> Furthermore, an increase in ultrasonic power contributes to higher mixing intensity due to the turbulence and microstreaming which are generated during the cavitational microbubble collapse,<sup>23</sup> which can also contribute to increased PRX degradation rates.

Figure 2.

### **3.3 Effect of bulk temperature**

Experiments were performed at 20 °C, 40 °C and 60 °C in order to study the effect of temperature on the degradation of 320 µg/L PRX at 36 W/L power density. Results in Figure 3 show that an increase in bulk temperature can reduce process efficiency, and therefore total degradation of PRX is achieved after about 10, 20 and 40 min of sonochemical treatment at 20 °C, 40 °C and 60 °C, respectively. Temperature of the bulk liquid can affect several parameters such as the vapor pressure, viscosity, gas solubility and surface tension. Therefore, the negative effect of temperature on PRX degradation may be explained by the following: the increase in temperature increases the vapor pressure of the solvent. Consequently, the cavitation bubbles contain more water vapor. Because of this increased vapor content, the collapse of the cavitation bubbles is less violent, which is known as the ‘cushioning effect’. This causes a reduction in the collapse temperature and thus a reduced production of •OH radicals. In addition to this, increased temperatures are likely to favour

degassing of the liquid phase, thus reducing the number of gas nuclei available for bubble formation.<sup>20,24</sup>

Figure 3.

### 3.4 Effect of the water matrix

The complexity of the water matrix is another operating parameter that can affect process efficiency. To assess its effect, experiments were conducted in surface water (SW), bottled water (BW), as well as in UPW spiked with humic acid (HA) at two concentrations (5 and 10 mg/L); in all cases, PRX concentration was 320 µg/L and the power density 36 W/L at 20 °C. Results in Figure 4 show that there is a decrease in the degradation rate in the presence of HA, BW and SW compared to that of UPW. This may be attributed to the fact that HA, BW, and SW contain other organic or inorganic substances that can act as hydroxyl radical scavengers and can therefore significantly lower the degradation of the target contaminant<sup>25</sup>. Specifically, PRX degradation is found to decrease in the order: UPW (0.2098 min<sup>-1</sup>) > 5 mg/L HA (0.1005 min<sup>-1</sup>) > BW (0.0819 min<sup>-1</sup>) > 10 mg/L HA (0.0706 min<sup>-1</sup>) > SW (0.0646 min<sup>-1</sup>) with numbers in brackets corresponding to kinetic rate coefficient. The lower degradation rates in the presence of HA, a model natural organic matter (NOM), may be due to the much higher concentration of organic carbon in the solution (5–10 mg/L HA versus 320 µg/L PRX), which competes with the substrate for the oxidative species<sup>26</sup>. Moreover, it is observed that increase of the initial HA concentration, from 5 to 10 mg/L, negatively affects PRX degradation, since the amount of the organics competing with PRX is higher at 10 mg/L than at 5 mg/L HA. PRX degradation in SW, which is the most complex

matrix studied, since it consists of NOM and several inorganic substances, is found to be lower than in all other water matrices. Therefore, results indicate that when the complexity of the water matrix is increased process efficiency is decreased.

Figure 4.

The presence of chlorides and bicarbonates in BW and SW partially impedes degradation since inorganics can scavenge hydroxyl radicals<sup>26</sup>. This was further demonstrated by performing experiments in UPW spiked with chlorides, in the form of NaCl, and sodium bicarbonate for degrading 320 µg/L PRX at 36 W/L power density and 20 °C. As shown in Figure 5, PRX degradation rate is substantially decreased in the presence of 250-500 mg/L NaCl as well as of 50-250 mg/L BIC. Results from this work are in agreement with previous studies dealing with the sonochemical degradation of drugs. For example, Xiao et al.<sup>11</sup> found that in the presence of terephthalate (TA), a typical •OH scavenger and dissolved Suwannee river fulvic acid (SRFA) the degradation rates of ciprofloxacin and ibuprofen are significantly reduced compared to no TA or SRFA present. Moreover, Gao et al.<sup>22</sup> reported that sulfamethoxazole degradation was inhibited in the presence of  $\text{NO}_3^{-1}$ ,  $\text{Cl}^{-}$  and  $\text{SO}_4^{-2}$  and the inhibition degree followed the order of  $\text{NO}_3^{-1}$ ,  $\text{Cl}^{-}$   $>$   $\text{SO}_4^{-2}$ .

Figure 5.

### 3.5 Identification of transformation by-products (TBPs) and degradation pathways

Simultaneously with PRX degradation, the formation and subsequent degradation of 14 TBPs was revealed. Structural assignment was based on high resolution accurate mass measurements in both positive and negative ionization mode (Tables 1 and 2). Firstly, under negative ionization mode PRX presents a molecular ion peak  $[M-H]^-$  at  $m/z$  330.0554 and fragments (isCID MS) at  $m/z$  266.0922 and 210.0224, which correspond to the loss of  $-SO_2$  followed intramolecular rearrangement and loss of pyridinecarboxamide moiety, respectively. The fragment ion at  $m/z$  146.0602 is generated by the loss of  $-SO_2$  followed intramolecular rearrangement from the 210.0224 fragment ion. Three TBPs (TBP 9, 10, 12) with molecular ions at  $m/z$  346.0493-346.0506 that differ about 16 amu from the PRX are identified as hydroxylated derivatives. Pyridine, benzothiazine moieties and N-methyl group can be considered as potential sites of hydroxylation. TBP 12 shows a fragment at  $m/z$  226.0180 which corresponds to the loss of pyridinecarboxamide moiety indicating that hydroxylation takes place at the benzothiazine moiety or N-methyl group. On the other hand, TBP 9 and 10 show close retention times but no diagnostic fragments. However, the hydroxylation of PRX molecule in the pyridinyl ring and more specifically at the 5'-position can be proposed for one of the isomeric TBPs since 5'-hydroxypiroxicam is reported as a well-known metabolite of PRX in the literature.<sup>28</sup>

In addition, two di-hydroxylated TBPs (TBP 6 and 11) are detected on the basis of +32 amu difference from the PRX molecule. TBP 11 shows a characteristic diagnostic fragment at  $m/z$  210.0224 corresponding to the loss of  $C_6H_4N_2O_3$  suggesting that hydroxylation takes place on the pyridinyl ring. Four isomeric TBPs (TBP 4, 5, 7, 8) with  $m/z$  212.0015-212.0030 and TBP 3 are proposed as the mono- and di-hydroxylatedbenzothiazine derivatives, respectively. Finally, TBPs 1, 2, 13 and 14 are identified as 1,2-benzisothiazol-3(2H)-one-1,1-dioxide, N-methyl-

240 benzenesulfonamide, N1-(pyridin-2-yl)oxalamide and N1-methyl-N2-(pyridin-2-yl)oxalamide.  
241 The profiles (peak area vs irradiation time) of the TBPs are shown in Figure 6. The sequence of  
242 the PRX transformation paths can be proposed based on the time within the maximum  
243 concentration of each TBP is observed. Therefore, TBPs 9, 10 and 12 (mono-hydroxy-TBPs)  
244 peaked up at 120 min allows us to consider them as first-stages TBPs. Di-hydroxylated-PRX  
245 derivatives (TBPs 6 and 11) and mono-, di-hydroxylated benzothiazine derivatives (TBPs 4, 5, 7  
246 and 8) peaked up at 180 min can be considered as secondary products. Finally, TBPs 1, 2, 13 and  
247 14 are detected only in samples after 240 min of treatment and at low concentration levels and thus  
248 they can be considered as later stage products. For the sake of comparison with other studies  
249 dealing with the degradation of PRX, TBP 14 and structurally similar TBPs have been also  
250 identified as degradation products of PRX under oxidative and photolytic conditions.<sup>29-32</sup> In  
251 addition, the in vivo formation of the metabolic oxidation product 5-hydroxypiroxicam and at least  
252 13 new secondary peaks (without structure identification) after the in vitro study of hydroxyl  
253 radical attack of PRX was reported elsewhere.<sup>33</sup>

254 Taking into account the identification and structural assignment of the TBPs, as well as their  
255 evolution profiles, the sonochemical degradation mechanisms of PRX are proposed in Figure 7.  
256 The first steps of degradation start with hydroxyl radical attack on PRX molecule leading to the  
257 formation of hydroxylated, di-hydroxylated derivatives. In parallel, apart from the generation and  
258 attack of hydroxyl radicals, singlet oxygen ( $^1\text{O}_2$ ) can be also formed in ample amounts <sup>34</sup> during  
259 the ultrasound treatment. PRX quenches  $^1\text{O}_2$  with rate constants in the order of  $10^8 \text{ M}^{-1} \text{ s}^{-1}$  showing  
260 a significant photodegradation efficiency, as reported elsewhere.<sup>35</sup> This pathway proceeds by the  
261 addition of singlet oxygen to the enol double bond and the formation of a dioxetane intermediate.  
262 Ring cleavage of this unstable intermediate, leads to its conversion in a carboxylic acid structure,

as depicted in Figure 7<sup>29,30,32</sup>, which is further transformed to later stages TBPs, such as TBP 1, 2, 13 and 14. The same degradation mechanism was proposed for the photochemical oxidation of PRX.<sup>29,30,32</sup>

#### 4. Conclusions

The aim of this work was to investigate the sonochemical degradation of piroxicam (PRX), a commonly used non-steroidal anti-inflammatory drug. For this purpose, the effect of key operating parameters was evaluated. The following parameters, namely initial PRX concentration, ultrasound power density, temperature, water matrix, and treatment time were studied. Transformation by-products were identified and a potential degradation pathway was identified. The main findings drawn from this study are summarized below.

- An increase of power density leads to enhanced PRX degradation rates, since at high power densities the amount of hydroxyl radicals generated and the mixing intensity are increased.
- Increasing the temperature of the bulk liquid results in a reduction of sonochemical activity and this may be attributed to the ‘cushioning’ phenomenon.
- Water matrices containing organic and inorganic radical scavengers can have adverse effect on degradation kinetics compared to runs in ultrapure water. Also, when the complexity of the water matrix is increased process efficiency is decreased.
- Sonochemical degradation starts with hydroxyl radical attacking on PRX molecule leading to the formation of hydroxylated and di-hydroxylated derivatives. At the same time, singlet oxygen is added to the enol double bond, thus leading to the formation of a dioxetane

284 intermediate, which is consequently converted to a carboxylic acid structure and other later  
285 stages transformation by-products.

286 In general ultrasound irradiation seems a promising technology with relative high efficiency (i.e  
287 removal of hundreds of  $\mu\text{g/L}$  in less than few minutes) for the destruction of micro pollutants.  
288 Further research is needed with particular emphasis at the scale up of the process in order to study  
289 the industrial application of sonochemistry in environmental protection.

290

291



## References

1. Lolić A, Paíga P, Santos LHMLM, Ramos S, Correia M and Delerue-Matos C, Assessment of non-steroidal anti-inflammatory and analgesic pharmaceuticals in seawaters of North of Portugal: Occurrence and environmental risk. *Sci Total Environ* **508**: 240–250 (2015).
2. Mainero Rocca L, Gentili A, Caretti F, Curini R and Pérez-Fernández V, Occurrence of non-steroidal anti-inflammatory drugs in surface waters of Central Italy by liquid chromatography–tandem mass spectrometry. *Int J Environ Anal Chem* **95**: 685–697 (2015).
3. Ziyilan A and Ince NH, The occurrence and fate of anti-inflammatory and analgesic pharmaceuticals in sewage and fresh water: Treatability by conventional and non-conventional processes. *J Hazard Mater* **187**: 24–36 (2011).
4. Bácsi I, B-Béres V, Kókai Z, Gonda S, Novák Z, Nagy SA and Vasas G, Effects of non-steroidal anti-inflammatory drugs on cyanobacteria and algae in laboratory strains and in natural algal assemblages. *Environ Pollut* **212**: 508–518 (2016).
5. Tran N, Drogui P and Brar SK, Sonochemical techniques to degrade pharmaceutical organic pollutants. *Environ Chem Lett* **13**: 251–268 (2015).
6. Tran N, Drogui P and Brar SK, Sonoelectrochemical oxidation of carbamazepine in waters: optimization using response surface methodology. *J Chem Technol Biotechnol* **90**: 921–929 (2015).
7. Ma X, Tang K, Li Q, Song Y, Ni Y and Gao N, Parameters on 17 $\beta$ -Estradiol degradation by Ultrasound in an aqueous system. *J Chem Technol Biotechnol* **89**: 322–327 (2014).

- 312 8. Darsinou B, Frontistis Z, Antonopoulou M, Konstantinou I and Mantzavinos D, Sono-  
313 activated persulfate oxidation of bisphenol A: Kinetics, pathways and the controversial role  
314 of temperature. *Chem Eng J* **280**: 623–633 (2015).
- 315 9. Oztekin R and Sponza DT, Treatment of wastewaters from the olive mill industry by  
316 sonication. *J Chem Technol Biotechnol* **88**: 212–225 (2013).
- 317 10. Méndez-Arriaga F, Torres-Palma RA, Pétrier C, Esplugas S, Gimenez J and Pulgarin C,  
318 Ultrasonic treatment of water contaminated with ibuprofen. *Water Res* **42**: 4243–4248  
319 (2008).
- 320 11. Xiao R, He Z, Diaz-Rivera D, Pee GY and Weavers LK, Sonochemical degradation of  
321 ciprofloxacin and ibuprofen in the presence of matrix organic compounds. *Ultrason*  
322 *Sonochem* **21**: 428–435 (2014).
- 323 12. Im J-K, Heo J, Boateng LK, Her N, Flora JRV, Yoon J, Zoh KD and Yoon Y, Ultrasonic  
324 degradation of acetaminophen and naproxen in the presence of single-walled carbon  
325 nanotubes. *J Hazard Mater* **254**: 284–292 (2013).
- 326 13. Ziylan A, Koltypin Y, Gedanken A and Ince NH, More on sonolytic and sonocatalytic  
327 decomposition of Diclofenac using zero-valent iron. *Ultrason Sonochem* **20**: 580–586  
328 (2013).
- 329 14. Güyer GT and Ince NH, Degradation of diclofenac in water by homogeneous and  
330 heterogeneous sonolysis. *Ultrason Sonochem* **18**: 114–119 (2011).

- 331 15. Naddeo V, Landi M, Scannapieco D and Belgiorno V, Sonochemical degradation of twenty-  
332 three emerging contaminants in urban wastewater. *Desalin Water Treat* **51**: 6601–6608  
333 (2013).
- 334 16. Naddeo V, Belgiorno V, Kassinos D, Mantzavinos D and Meric S, Ultrasonic degradation,  
335 mineralization and detoxification of diclofenac in water: Optimization of operating  
336 parameters. *Ultrason Sonochem* **17**: 179–185 (2010).
- 337 17. Feng L, Watts MJ, Yeh D, Esposito G and van Hullebusch ED, The Efficacy of Ozone/BAC  
338 Treatment on Non-Steroidal Anti-Inflammatory Drug Removal from Drinking Water and  
339 Surface Water. *Ozone Sci Eng* **37**: 343–356 (2015).
- 340 18. Madhavan J, Grieser F and Ashokkumar M, Combined advanced oxidation processes for  
341 the synergistic degradation of ibuprofen in aqueous environments. *J Hazard Mater* **178**:  
342 202–208 (2010).
- 343 19. Madhavan J, Kumar PSS, Anandan S, Zhou M, Grieser F and Ashokkumar M, Ultrasound  
344 assisted photocatalytic degradation of diclofenac in an aqueous environment. *Chemosphere*  
345 **80**: 747–752 (2010).
- 346 20. Psillakis E, Mantzavinos D and Kalogerakis N, Monitoring the sonochemical degradation  
347 of phthalate esters in water using solid-phase microextraction. *Chemosphere* **54**: 849–857  
348 (2004).

- 349 21. Torres RA, Pétrier C, Combet E, Carrier M and Pulgarin C, Ultrasonic cavitation applied to  
350 the treatment of bisphenol A. Effect of sonochemical parameters and analysis of BPA by-  
351 products. *Ultrason Sonochem* **15**: 605–611 (2008).
- 352 22. Gao Y, Gao N, Deng Y, Gu J, Gu Y and Zhang D, Factors affecting sonolytic degradation  
353 of sulfamethazine in water. *Ultrason Sonochem* **20**: 1401–1407 (2013).
- 354 23. Mowla A, Mehrvar M and Dhib R, Combination of sonophotolysis and aerobic activated  
355 sludge processes for treatment of synthetic pharmaceutical wastewater. *Chem Eng J* **255**:  
356 411–423 (2014).
- 357 24. Emery RJ, Papadaki M, Freitas dos Santos LM and Mantzavinos D, Extent of sonochemical  
358 degradation and change of toxicity of a pharmaceutical precursor (triphenylphosphine  
359 oxide) in water as a function of treatment conditions. *Environ Int* **31**: 207–211 (2005).
- 360 25. Gogate R, Mujumdar S, Pandit A, Sonochemical reactors for waste water treatment:  
361 comparison using formic acid degradation as a model reaction *Adv Environ Res* **7**:283-299  
362 (2003).
- 363 26. Rayaroth M, Aravind U, Aravindakumar T, Sonochemical degradation of Coomassie  
364 Brilliant Blue: Effect of frequency, power density, pH and various additives. *Chemosphere*  
365 **119**: 848-855 (2015).
- 366 27. Guzman-Duque F, Petrier C, Pulgarin C, Penueal G, Torres-Palma R, Effects of  
367 sonochemical parameters and inorganic ions during the sonochemical degradation of crystal  
368 violet in water. *Ultrason Sonochem* **18**:440-446 (2011).

- 369 28. McKinney AR, Suann CJ and Stenhouse AM, The detection of piroxicam, tenoxicam and  
370 their metabolites in equine urine by electrospray ionisation ion trap mass spectrometry.  
371 *Rapid Commun Mass Spectrom* **18**: 2338–2342 (2004).
- 372 29. Glass BD, Brown ME, Daya S, Worthington MS, Drummond P, Antunes E, Lebete M,  
373 Anoopkumar-Dukie M and Maharaj D, Influence of cyclodextrins on the photostability of  
374 selected drug molecules in solution and the solid-state. *Int J Photoenergy* **3**: 205–211  
375 (2001).
- 376 30. Modhave DT, Handa T, Shah RP and Singh S, Successful characterization of degradation  
377 products of drugs using LC-MS tools: Application to piroxicam and meloxicam. *Anal*  
378 *Methods* **3**: 2864 (2011).
- 379 31. Tománková H and Šabartová J, Determination of potential degradation products of  
380 piroxicam by HPTLC densitometry and HPLC. *Chromatographia* **28**: 197–202 (1989).
- 381 32. Ilic-Stojanovic S, Nikolic V, Nikolic L, Zdravkovic A, Kapor A, Popsavin M and Petrovic  
382 D, The improved photostability of naproxen in the inclusion complex with 2-  
383 hydroxypropyl- $\beta$ -cyclodextrin. *Hem Ind* **69**: 361–370 (2015).
- 384 33. Gaudiano M., Valvo L, Bertocchi P and Manna L, RP-HPLC study of the degradation of  
385 diclofenac and piroxicam in the presence of hydroxyl radicals. *J Pharm Biomed Anal* **32**:  
386 151–158 (2003).

34. Matsumura Y, Iwasawa A, Kobayashi T, Kamachi T, Ozawa T and Kohno M, Detection of High-frequency Ultrasound-induced Singlet Oxygen by the ESR Spin-trapping Method *Chem Lett* **42**: 1291–1293 (2013).
35. Ferrari G V., Natera J, Paulina Montaña M, Muñoz V, Gutiérrez EL, Massad W, Miskoski S and Garcia NA, Scavenging of photogenerated ROS by Oxicams. Possible biological and environmental implications. *J Photochem Photobiol B Biol* **153**: 233–239 (2015).

396 **List of Tables**

397 **Table 1.** High resolution accurate LC-MS data for PRX and identified TBPs in negative ionization  
398 mode (\*TBPs detected also in positive ionization mode).

399 **Table 2.** High resolution accurate LC-MS data for PRX and identified TBPs in positive ionization  
400 mode (\*TBPs detected also in negative ionization mode).

401

402 **Table 1.**

TBP code	R <sub>t</sub> (min)	Deprotonated molecular formula	m/z [M-H] <sup>-</sup>	Δ (ppm)	RDBe
TBP1	4.4	C <sub>7</sub> H <sub>4</sub> NO <sub>3</sub> S	181.9925	-4.0	6.5
TBP2	4.7	C <sub>7</sub> H <sub>8</sub> NO <sub>2</sub> S	170.0276	3.2	4.5
TBP3	5.1	C <sub>8</sub> H <sub>6</sub> NO <sub>5</sub> S	227.9972	-1.2	6.5
TBP4	5.4	C <sub>8</sub> H <sub>6</sub> NO <sub>4</sub> S	212.0030	-3.4	6.5
TBP5	6.0	C <sub>8</sub> H <sub>6</sub> NO <sub>4</sub> S	212.0021	0.9	6.5
TBP6*	6.1	C <sub>15</sub> H <sub>12</sub> N <sub>3</sub> O <sub>6</sub> S	362.0452	0	11.5
TBP7	6.3	C <sub>8</sub> H <sub>6</sub> NO <sub>4</sub> S	212.0026	-1.2	6.5
TBP8	6.6	C <sub>8</sub> H <sub>6</sub> NO <sub>4</sub> S	212.0015	4.0	6.5
TBP9*	6.9	C <sub>15</sub> H <sub>12</sub> N <sub>3</sub> O <sub>5</sub> S	346.0493	3.0	11.5
		C <sub>15</sub> H <sub>12</sub> N <sub>3</sub> O <sub>3</sub>	282.0875	3.3	11.5
TBP10*	7.1	C <sub>15</sub> H <sub>12</sub> N <sub>3</sub> O <sub>5</sub> S	346.0494	2.7	11.5
		C <sub>15</sub> H <sub>12</sub> N <sub>3</sub> O <sub>3</sub>	282.0875	3.3	11.5
PRX	7.2	C <sub>15</sub> H <sub>12</sub> N <sub>3</sub> O <sub>4</sub> S	330.0554	0	11.5
		C <sub>15</sub> H <sub>12</sub> N <sub>3</sub> O <sub>2</sub>	266.0922	4.9	11.5
		C <sub>9</sub> H <sub>8</sub> NO <sub>3</sub> S	210.0224	2.9	6.5
		C <sub>9</sub> H <sub>8</sub> NO	146.0602	6.6	6.5
TBP11*	7.6	C <sub>15</sub> H <sub>12</sub> N <sub>3</sub> O <sub>6</sub> S	362.0450	0.7	11.5
		C <sub>15</sub> H <sub>12</sub> N <sub>3</sub> O <sub>2</sub>	266.0922	4.9	11.5
		C <sub>9</sub> H <sub>8</sub> NO <sub>3</sub> S	210.0224	2.9	6.5
		C <sub>9</sub> H <sub>8</sub> NO	146.0602	6.6	6.5
TBP12*	8.0	C <sub>15</sub> H <sub>12</sub> N <sub>3</sub> O <sub>5</sub> S	346.0506	-0.8	11.5
		C <sub>9</sub> H <sub>8</sub> NO <sub>4</sub> S	226.0180	-1.4	6.5

403



404 **Table 2.**

<b>TBP code</b>	<b>R<sub>t</sub> (min)</b>	<b>Protonated molecular formula</b>	<b>m/z [M+H]<sup>+</sup></b>	<b>Δ (ppm)</b>	<b>RDBe</b>
TBP13	5.8	C <sub>7</sub> H <sub>8</sub> N <sub>3</sub> O <sub>2</sub>	166.0615	-2.4	5.5
TBP14	6.4	C <sub>8</sub> H <sub>10</sub> N <sub>3</sub> O <sub>2</sub>	180.0775	-3.9	5.5
TBP6*	6.1	C <sub>15</sub> H <sub>14</sub> N <sub>3</sub> O <sub>6</sub> S	364.0591	1.9	10.5
TBP9*	6.9	C <sub>15</sub> H <sub>14</sub> N <sub>3</sub> O <sub>5</sub> S	348.0650	-0.3	10.5
TBP10*	7.1	C <sub>15</sub> H <sub>14</sub> N <sub>3</sub> O <sub>5</sub> S	348.0651	-0.7	10.5
PRX	7.2	C <sub>15</sub> H <sub>14</sub> N <sub>3</sub> O <sub>4</sub> S	332.0687	3.9	10.5
TBP11*	7.6	C <sub>15</sub> H <sub>14</sub> N <sub>3</sub> O <sub>6</sub> S	364.0595	0.8	10.5
TBP12*	8.0	C <sub>15</sub> H <sub>14</sub> N <sub>3</sub> O <sub>5</sub> S	348.0650	-0.3	10.5

405

406

## List of Figures

**Figure 1.** Effect of initial PRX concentration on its sonochemical degradation at 36 W/L power density with temperature control at 20 °C. Inset graph: Reaction rate coefficient as a function of initial PRX concentration.

**Figure 2.** Effect of power density on sonochemical degradation of 640 µg/L PRX with temperature control at 20 °C. Inset graph: Reaction rate coefficient as a function of power density.

**Figure 3.** Effect of temperature on sonochemical degradation of 320 µg/L PRX at 36 W/L power density.

**Figure 4.** Effect of the water matrix on sonochemical degradation of 320 µg/L PRX sonodegradation at 36 W/L power density with temperature control at 20 °C.

**Figure 5.** Effect of (a) NaCl, and (b) bicarbonate (BIC) on the sonochemical degradation of 320 µg/L PRX at 36 W/L power density with temperature control at 20 °C.

**Figure 6.** Formation and degradation kinetics of identified TBPs under ultrasonic radiation.

**Figure 7.** Sonochemical degradation pathways of PRX.

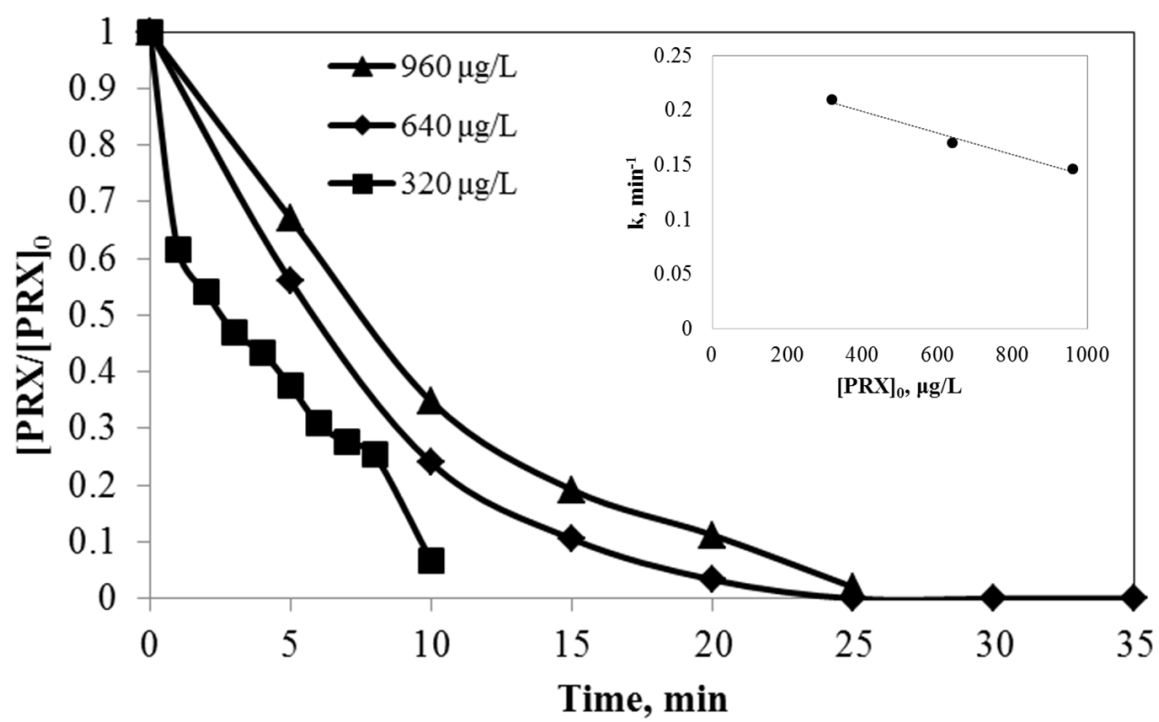


Figure 1

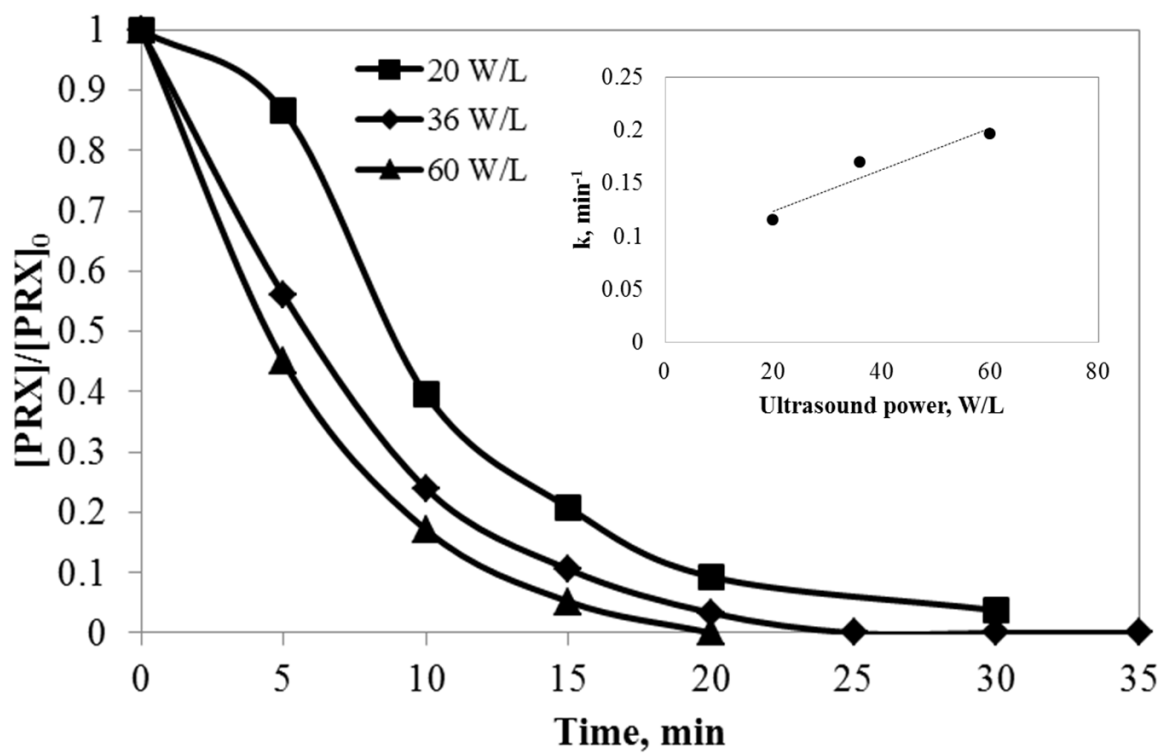


Figure 2

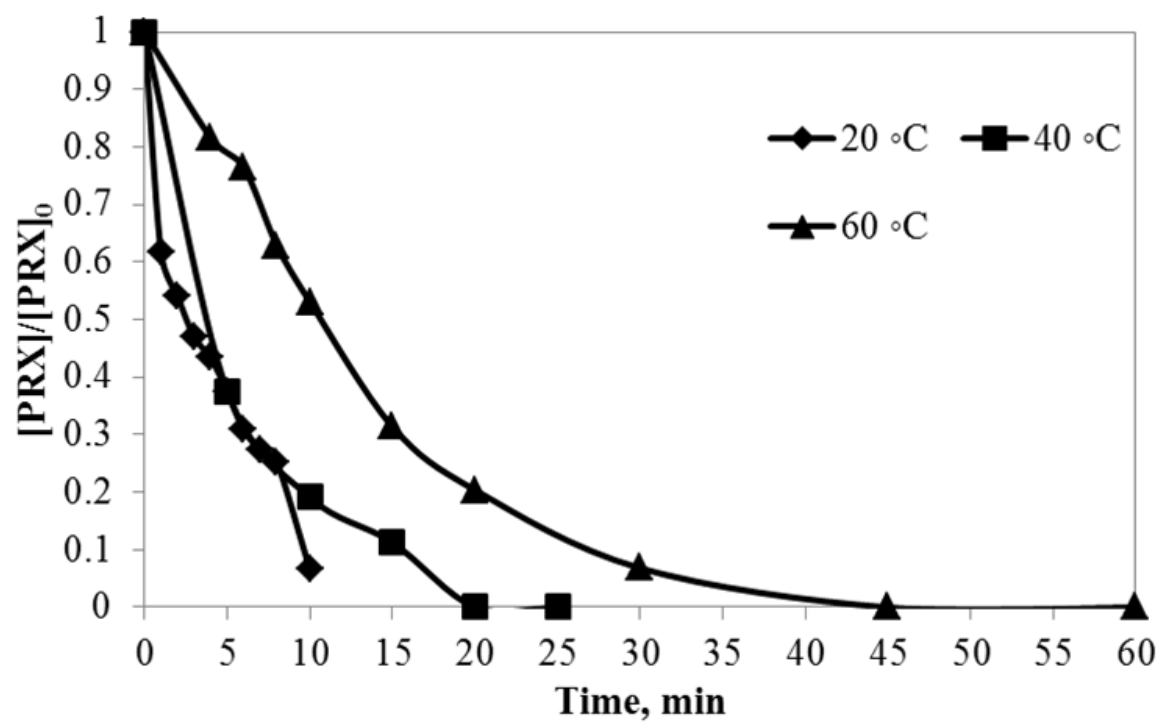


Figure 3

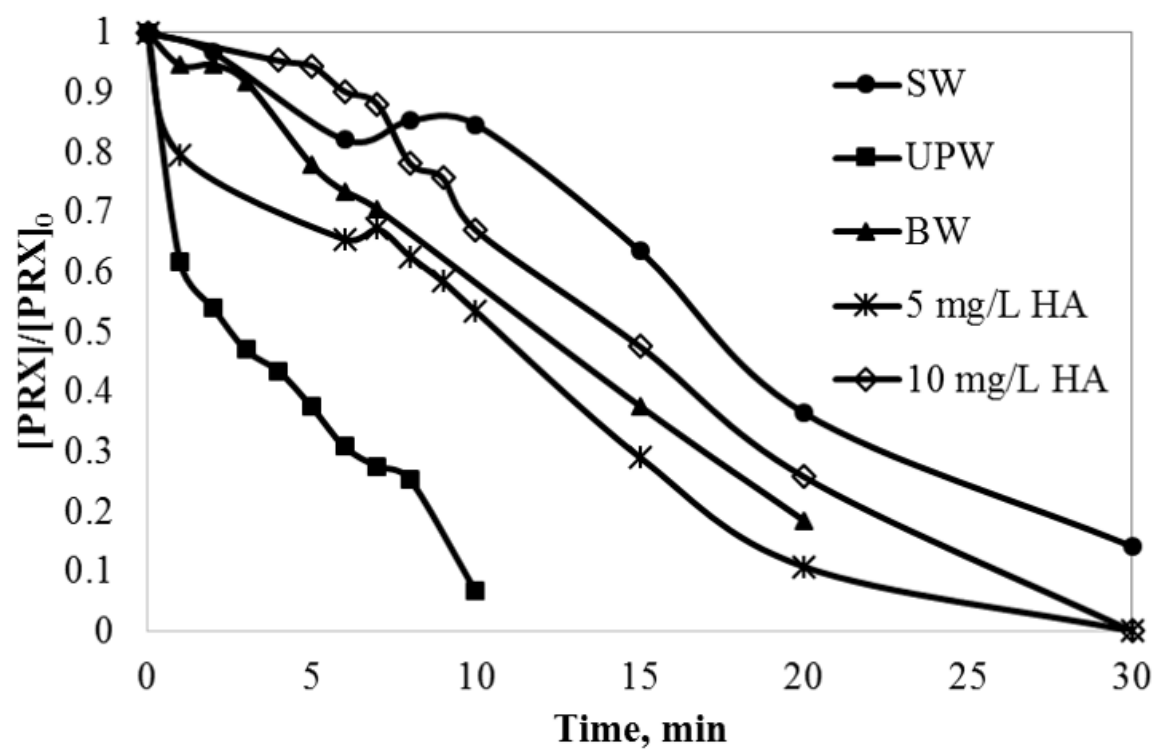
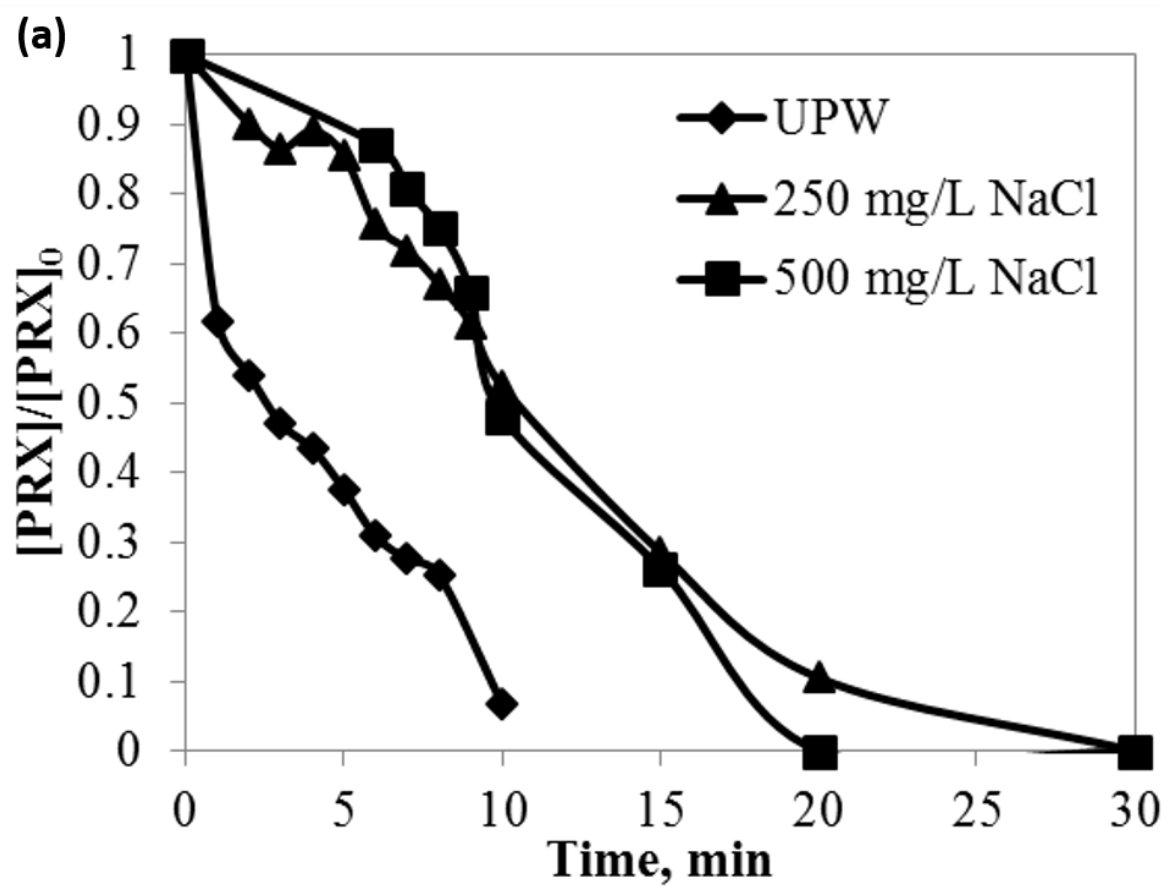


Figure 4



447

448

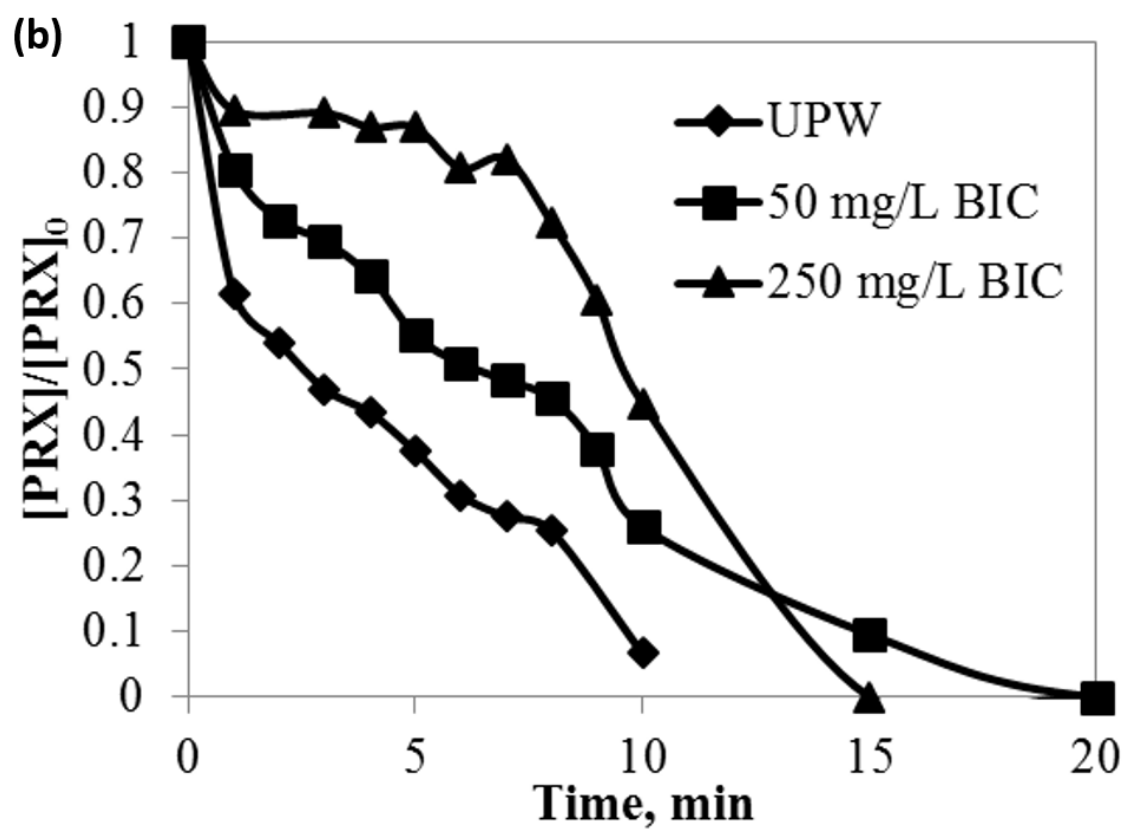


Figure 5



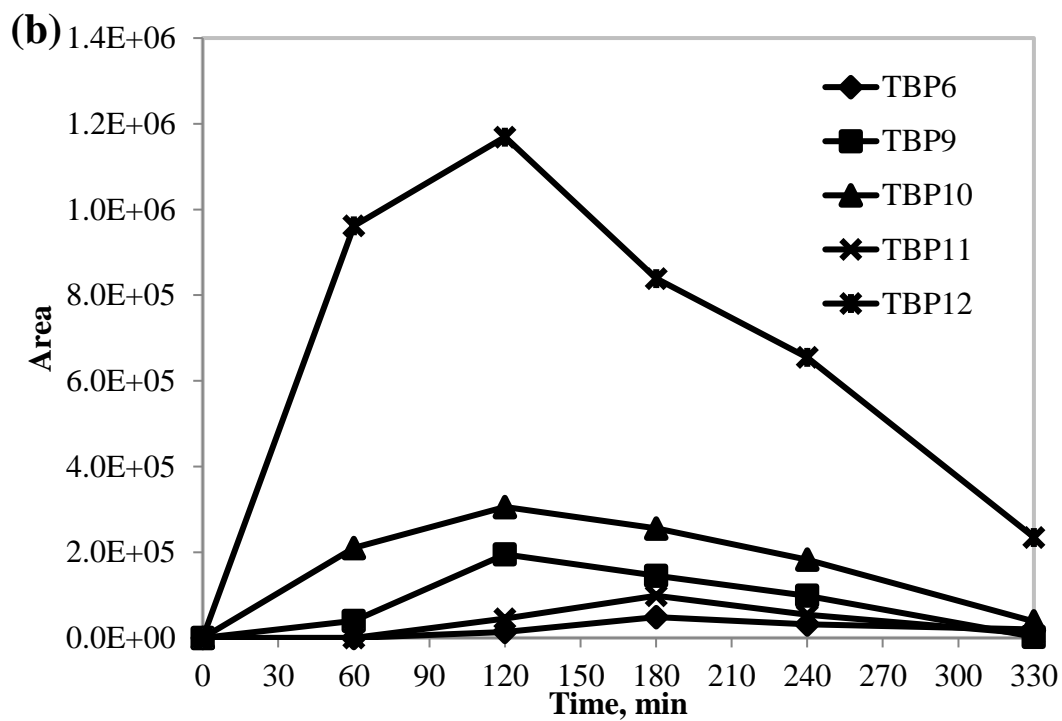
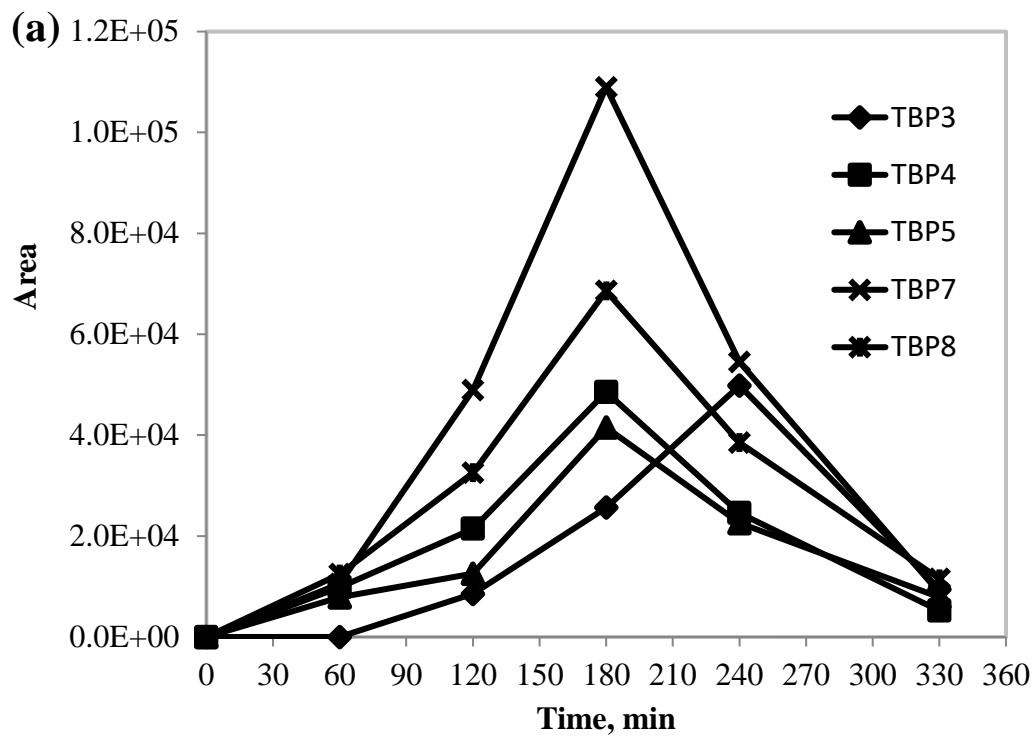
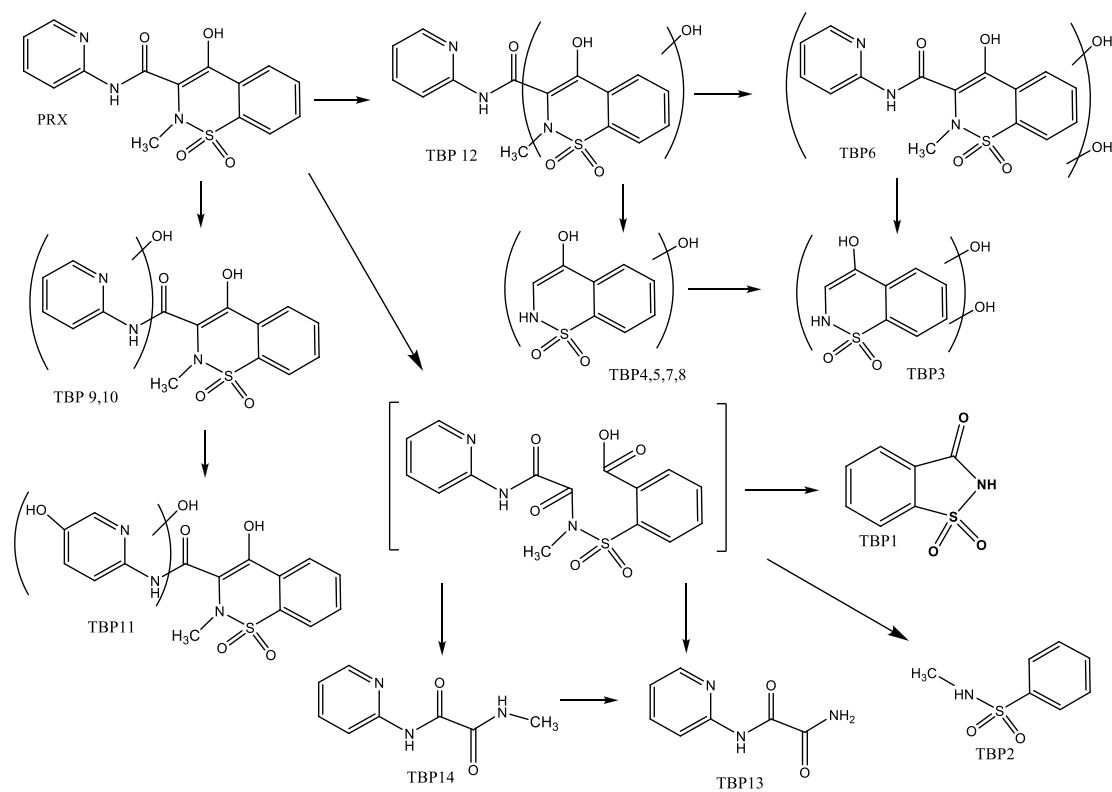


Figure 6

455

456



457

458 Figure 7

459